886

APPLICATION OF LOW ALTITUDE PHOTOGRAMMETRY TO THE DETERMINATION OF RANGELAND HYDRAULIC PARAMETERS

C. E. C. Drungil, R. H. McCuen, J. R. Simanton
MEMBER
ASAE

ABSTRACT

The physically based erosion model developed by the Water Erosion Prediction Project (WEPP) of the USDA requires input data that are not routinely measured or estimated in the field. Low altitude photogrammetry data were collected at 12 rangeland locations to measure surface micro-elevations needed to estimate hydraulic geometries of the flow. The photogrammetry contour data were converted to cross-sections, and used to calculate the hydraulic geometries and flowpath density on each cross section. The erosion prediction segment of the WEPP model was optimized with the photogrammetrically derived parameters used as input. The low-altitude photogrammetry makes the measurement of surface hydraulic properties possible on low-relief rangelands resulting in more accurate soil erosion predictions.
KEYWORDS. Erosion, Photogrammetry, Rangeland runoff, WEPP model.

INTRODUCTION

Erosion on rangelands, which comprises approximately 40% of U.S. land, is an important concern. However until recently, progress on understanding erosion on rangelands has been hindered by the lack of an adequate data base. This data base has dramatically expanded since 1985 as a part of the USDA-Water Erosion Prediction Project (WEPP) that is developing a replacement for the Universal Soil Loss Equation (Wischmeier and Smith, 1978) based on fundamental hydrologic and erosion processes (Foster, 1987).

In this study, photogrammetric techniques were applied to low altitude photography to study the relationship between soil surface microtopography and erosion. The photogrammetric data should prove especially useful on rangelands where soil erosion often occurs at the microtopographic scale. On the rangeland plots evaluated in this study, the runoff flowpaths were shallow even under simulated heavy rainfall conditions. The accurate measurement of these shallow rangeland flowpaths requires the detail that these photogrammetric data provide.

The WEPP model (Nearing and Lane, 1989) requires a description of the flow channel geometry for input. Because of the importance of the channel geometry, data of various forms for channel geometry were collected as part of WEPP. The results of the analysis of the WEPP data for determining the hydraulic radius (R_h) of rangeland watersheds are reported.

The objectives of the study were to: (1) develop a procedure for transforming microtopographic-derived contour data into cross-sections for the WEPP experimental plots; (2) calibrate equations for predicting the hydraulic radius and rill spacing for rangeland watersheds; and (3) evaluate the accuracy of estimated erosion rates that incorporate the calibrated hydraulic radius equations.

BACKGROUND

THE HYDRAULIC RADIUS

The hydraulic radius is an important input to both surface erosion and channel erosion models for determining the shear stress exerted on the soil surface. The average shear stress in concentrated flow is computed by:

$$\tau = \gamma * R_h * S \qquad (1)$$

where

τ = average shear stress (N/m^2),
γ = specific weight of water (N/m^3),
R_h = hydraulic radius (m), and
S = slope.

The sediment transport capacity and detachment capacity of runoff are functions of the shear stress.

The hydraulic radius is a function of the flowpath or rill geometry. It not only varies with surface roughness, but also depends on the flow rate and velocity of runoff for a given surface profile. Nearing and Lane (1988) describe the first edition of the WEPP erosion model. This version assumes a rectangular flowpath geometry and estimates the flowpath dimensions when calculating the hydraulic radius. The width is given by:

$$w = a * Qe^{0.5} \qquad (2)$$

where

w = width (m),
Qe = discharge at the end of the slope (m^3/s), and a is:

$$a = 10.314/^{\tau} C^{0.5} \qquad (3)$$

Article was submitted for publication in June 1990; reviewed and approved for publication by the Soil and Water Div. of ASAE.

Contribution from USDA-ARS, Hydrology Laboratory, Beltsville, MD.

The authors are C. E. C. Drungil, Agricultural Engineer, USDA-ARS, Hydrology Laboratory, Beltsville, MD; R. H. McCuen, Professor, Dept. of Civil Engineering, University of Maryland, College Park; and J. R. Simanton, Hydrologist, USDA-ARS, Aridland Watershed Management Research Unit, Tucson, AZ.

where τ_c is the critical shear stress necessary for detachment (N/m^2).

The depth of flow is computed with an iterative technique based on the Chezy equations, which includes the friction factor of the flowpath, the flowpath width, and the slope gradient. The flowpath spacing is incorporated into these calculations. The hydraulic radius is then computed from the width and depth.

Rangeland Erosion and Rill Formation

Most investigations of surface roughness have been conducted on cropland soils under tillage conditions, with only limited work reported for rangelands. Sanchez and Wood (1987) examined roughness relationships on natural and reclaimed rangelands. Microtopography was measured with a point frame positioned both parallel (horizontal) and perpendicular (vertical) to the slope. The natural areas showed greater horizontal roughness because of rill formation, while the reclaimed pit-mined areas had greater vertical roughness caused by the establishment of vegetation that trapped sediment in overland flow.

A study of overland flow on rangeland plots by Emmett (1970) showed that most surface runoff travelled downslope in lateral concentrations of flow, but this was not considered rill flow. No observable rill formation took place at any of his field sites, even after extensive sprinkling. The individual flow patterns were dependent on the physical characteristics of the different slopes, such as mounds formed by rocks and vegetation.

Aerial Photography for Erosion Assessment

A photogrammetric technique similar to that used in this study was described by Welch et al. (1984). Stereo photographs were analyzed to obtain a network of X, Y, and Z coordinates, and a uniformly gridded digital terrain model was constructed through interpolation. The procedure provided a root mean square error (RMSE) value of about ±6 mm in elevation.

Several studies describe the assessment of gully erosion with aerial photogrammetry. Spomer and Mahurin (1984) used a truck-mounted camera at heights of 15 to 21 m to measure large relief gullies that had depths from 4.6 to 6.1 m. They obtained a ground elevation accuracy of ±0.02 m, which also permitted rill mapping and the accurate determination of total soil loss. Thomas et al. (1986) obtained vertical measurement accuracies of ±10 mm to ±25 mm with aerial photographs from 150 to 400 m above the terrain. Using a series of photographs from four periods during the year, they were able to measure soil erosion rates ranging from 1 to 32 m^3 from gullies approximately 0.04 ha in area with drainage areas of approximately 0.8 ha.

Dymond and Hicks (1986) measured erosion from a mountainous catchment using historical aerial photographs. From photographs taken at scales of 1:17500 and 1:12000 they created profiles and digital elevation models to describe the erosion scars and channel reaches. Ephemeral gully erosion was measured from stereo aerial photographs by Thomas and Welch (1988). Data were obtained from photographs recorded 300 m above the terrain, with vertical accuracies of ±25 mm and contour intervals of 0.15 m.

Methods

WEPP Rangeland Data Collection

The analysis is based on data collected during the spring and summer of 1987 at 18 sites at 12 locations throughout the western United States. These sites included a variety of conditions with ustic, xertic, and aridic moisture regimes, and mollisol, altisol, entisol, and inceptisol soil orders, as well as exhibiting variations in slope and vegetation.' Simanton et al. (1987) gave a complete description of the WEPP rangeland experiments.

A rainfall simulator (Swanson, 1965) was used to produce runoff and erosion on dry, wet, and very wet surfaces. To assess the surface roughness and any changes in the microtopography, low altitude photographs were collected for each plot. A truck-mounted camera obtained stereophoto pairs from 15 m above the plot. The photos were analyzed using photogrammetric techniques (Welch et al., 1984) at the University of Georgia Center for Remote Sensing and Mapping Science to create contour maps of the plots. The accuracy of the contour data is approximately 10 to 20 mm horizontally and 5 mm vertically.

Interpretation of the Photogrammetric Contour Maps

The final product of the WEPP photogrammetric analysis was a digital contour map of the experimental plot for the initial and final conditions. The contour interval was 50 mm, and each contour contained approximately 250 to 400 individual points across the 3-m wide plot. While the contour maps provided a good overview of the plot surfaces, it was difficult to make any flowpath measurements that could be used to compute values of hydraulic characteristics, such as an average hydraulic radius for the plot. Flowpaths could not be traced by visual inspection because clearly defined rilling patterns did not develop on the rangeland plots. Therefore, the initial task was to convert the digital contour data into a series of digital cross-sections on each plot.

The contour maps for the 3 m by 10 m plots indicated a relatively uniform slope along each plot. A method whereby a constant slope at each cross-section was assumed to be equal to the average slope along the entire plot allowed the cross-sections to be computed directly from the contours. As shown in figure 1(a), the X-value furthest downslope was chosen along each contour; this was used as the location of the estimated cross-section.

The horizontal distance between each point on the contour and the cross-section location was calculated. Given these horizontal distances and the plot slope, the vertical distances were calculated from simple geometry as demonstrated in figure 1(b). The vertical distance, when subtracted from the contour elevation, gives the elevation at that point along the new cross-section. Given the short distance between the contour and the cross-section, the cross-sections were assumed to be sufficiently accurate for making the necessary estimates of the hydraulic characteristics.

Sets of cross-sections derived directly from the photogrammetric data were obtained for two plots. They were assumed to be equivalent in accuracy to the contour data and representative of the true cross-sections. Figure 2 shows a typical cross-section from a plot in Cottonwood,

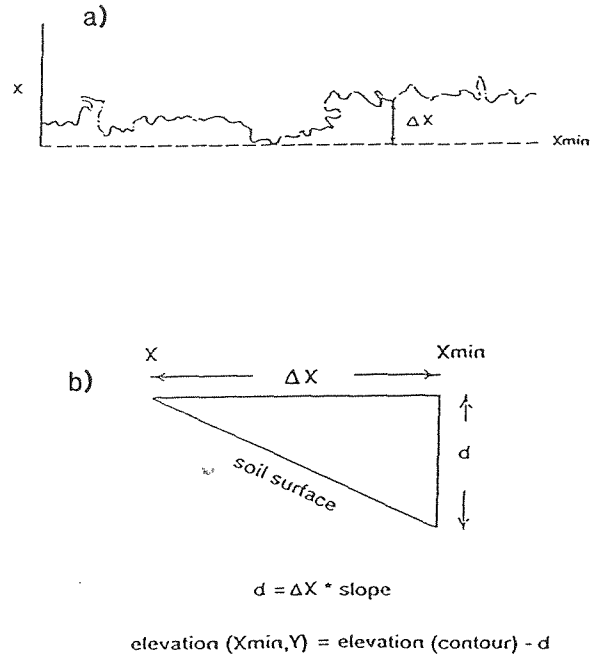

Figure 1–Conversion of contours to cross-sections calculate horizontal distances between contour and contour minimum, and geometrically determine vertical distances and compute elevations.

SD, plotted with both the photogrammetric and computed data points. Agreement is very good between the two cross-sections on the right-hand half of the plot. The computed section tends to lie above the photogrammetric section on the left-hand half perhaps because of a variation in slope on this part of the plot. However, noting the vertical scale, the differences are generally less than 10 mm.

Calculation of Flowpath Characteristics

Once the cross-sections were obtained for each plot, the flowpath characteristics of hydraulic radius and flowpath density, were computed as described by Drungil (1989).

Because the flowpath characteristics vary with the flow rate, the calculations were made for cross-sectional areas of flow ranging from 2000 to 20 000 mm^2. This range was chosen from an examination of the plot runoff data to include all measured flow rates. The trapezoidal rule was used to calculate flow areas in the cross-sections, which were assumed to fill from their minimum elevation. This assumption was considered best in the absence of plot photographs to verify actual flowpath locations. An iterative technique was used to adjust the flow level until the calculated flow area equaled the target flow area.

Once the elevation of the flow surface was calculated, the flow parameters could be computed. The wetted perimeter was first computed as the straight-line distance between all submerged points on the cross-section. A straight-line approximation was considered adequate with the given density of data points (approximately 1 point/10 mm). The flowpath density was the number of contour segments submerged by flow, and the flow width was the total submerged width of the cross-section. The hydraulic radius was computed as the flow area divided by the wetted perimeter. The maximum flow depth equaled the flow surface elevation minus the minimum cross-section elevation, and the average depth equaled the flow area divided by the flow width.

Results and Discussion

The photogrammetric analysis gave information about the entire plot surface, and the analysis described above provides the hydraulic parameters for each cross-section on a plot, as well as mean values for each plot. Figure 3 shows one cross-section for three flow depths, with the corresponding values of the associated flow area and hydraulic radius. The WEPP erosion model does not function at this level of detail; it requires only one value of the hydraulic radius and rill spacing for an entire plot or field. Therefore, it was necessary to compute the most representative value for a plot.

Several factors including the parameter variation within and between plots and the spatial and temporal variation of the parameters were considered. Analysis of variance tests

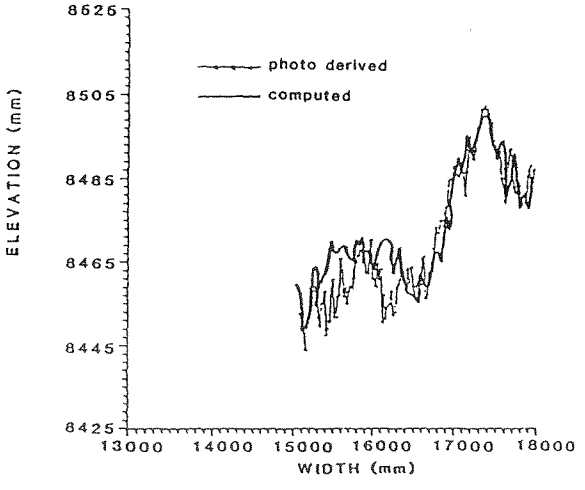

Figure 2–Comparison of a photo-derived and computed cross-section on plot 121, Cottonwood, SD.

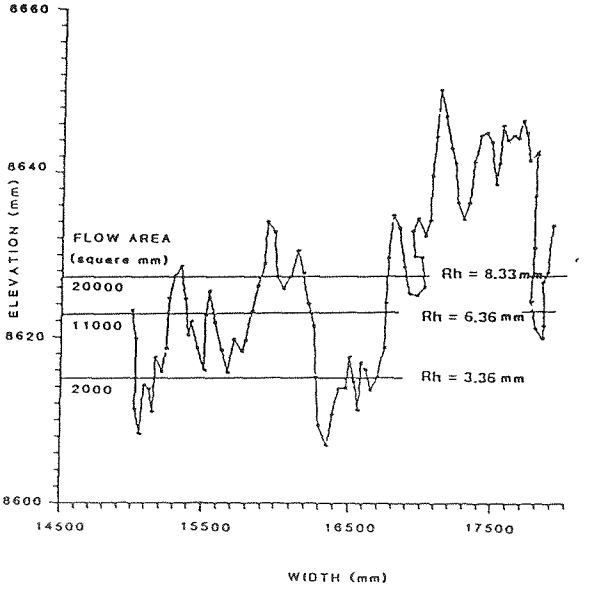

Figure 3–A cross-section from plot 121, Cottonwood, SD, showing the changing hydraulic parameters with increasing flow area.

showed that neither the hydraulic radius nor the flowpath density was spatially dependent. The mean difference, mean relative error, and bias between the initial and final values for both parameters were small. It was concluded that no significant difference existed between the values of the hydraulic parameters for the initial and final conditions. Therefore, a simple mean of the initial and final values for each cross-section of a plot was chosen as representative for both the hydraulic radius and the flowpath density.

The Flowpath Parameters as Functions of Flow Area

The values of the flowpath parameters will clearly change as the surface runoff rate changes. Variations in the runoff volume and velocity are reflected by the changing flow area in the cross-sections. The photogrammetric data provided average plot values of both the hydraulic radius and the flowpath density for a series of cross-sectional flow areas. However, to be applicable to all overland flow conditions, values of hydraulic radius and flowpath density must be available for any flow area. Functional relationships between both the hydraulic radius and the flowpath density and the flow area can be fitted so that values of the two parameters can be obtained for all flow areas.

The flow rate at each cross-section of a plot was estimated from the measured flow rate at the plot outlet and used with the velocity to estimate the depth of flow for each cross-section. Flow velocity measured on eight plots were used to develop a velocity estimation model for the remaining plots (Drungil, 1989). The hydraulic radius could then be determined given the depth of flow in each cross-section. Graphs of the hydraulic radius versus the flow area for the individual plots showed a smooth, curvilinear relationship that could be represented by a power model structure. A typical relationship is shown in figure 4. The data from each plot were used to develop power models for each plot (Table 1). An examination of the data in Table 1 shows a distinct linear relationship between the intercept and exponent coefficients; as the intercept coefficient increases, the exponent decreases. To test whether or not the computed correlation coefficient is significantly less than zero, critical values of the correlation coefficient for 16° of freedom and for a level of

TABLE 1. Parameters for the hydraulic radius-flow area model $R_h = bA^c$

WEPP plot	Location	b	c
31	Walnut Gulch, AZ	0.236	0.389
34	Walnut Gulch, AZ	0.216	0.369
72	Chickasha, OK	0.103	0.447
85	Woodward, OK	0.054	0.530
92	Woodward, OK	0.138	0.422
93	Woodward, OK	0.265	0.346
102	Sidney, MT	0.112	0.447
105	Sidney, MT	0.278	0.328
108	Meeker, CO	0.186	0.403
110	Meeker, CO	0.086	0.495
114	Cottonwood, SD	0.120	0.446
116	Cottonwood, SD	0.135	0.403
120	Cottonwood, SD	0.103	0.431
121	Cottonwood, SD	0.184	0.373
127	Los Alamos, NM	0.093	0.456
131	Cuba, NM	0.196	0.381
134	Cuba, NM	0.116	0.437
138	Susanville, CA	0.273	0.338

significance of 0.0005 is -0.71. Therefore, the sample R of -0.90 is highly significant. The sample correlation coefficient is sufficiently significant to justify estimating one parameter from the other, i.e., exponent = f(intercept).

In general, the graph of the flowpath density versus the flow area for each plot showed a curvilinear relationship similar to that evident with the hydraulic radius. However, the flowpath density data showed greater scatter, with several of the 18 plots showing very little association. Figure 5 is typical of the graphical results. A power model best described the density-area relationship. These model parameters (Table 2) varied considerable in magnitude and sign. An examination of the actual cross-sections revealed that the flowpath density did not increase (or decrease) systematically with increasing flow area as the hydraulic radius did. Very small depressions were counted as individual flowpaths flow areas, but combined to form a single path as the flow areas increased. But at larger flow areas, additional paths at higher elevations were also added, thus not changing the flowpath density.

The flowpath density values at the largest flow area (20 000 mm^2) were chosen as most representative of the actual density. With the large flow area, all of the identified paths should be sufficiently large to truly qualify as

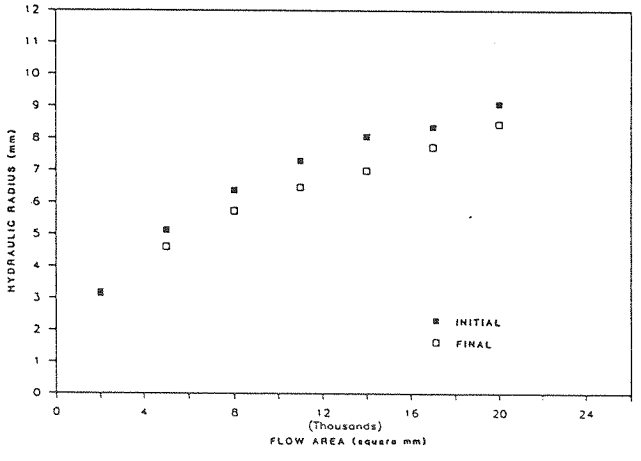

Figure 4–The hydraulic radius-flow area relationship for plot 134, Cuba, NM.

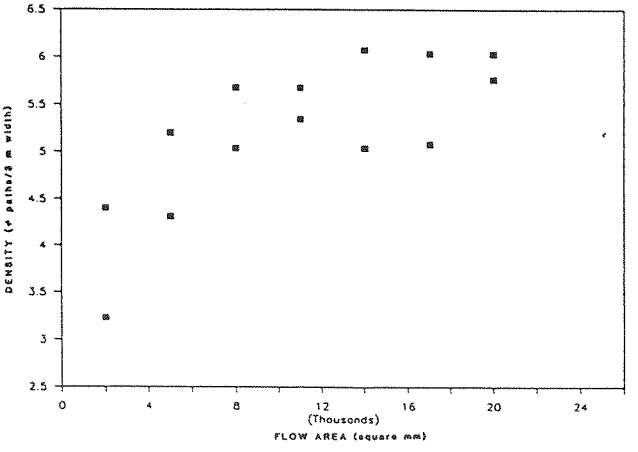

Figure 5–The flowpath density - flow area relationship for plot 121, Cottonwood, SD.

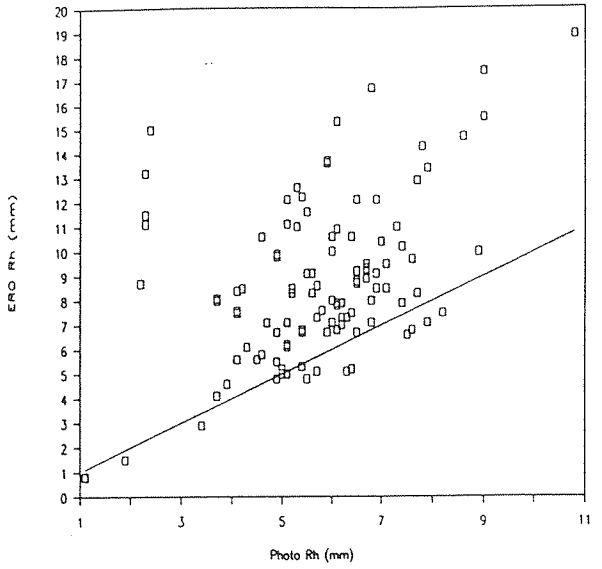

Figure 6–The WEPP model estimated hydraulic radius vs. the photo-derived hydraulic radius.

individual flowpaths. This flowpath density (number of flowpaths/3 m width) was converted to an average flowpath spacing (m) (Table 2) for each plot. The flowpath spacing is required input to the WEPP erosion model.

WEPP Erosion Model Results

The best test of the photogrammetry-derived flowpath parameters is their application in the WEPP erosion model and an assessment of the accuracy of the resulting erosion predictions. Numerical optimization was required to provide values of unmeasurable input parameters for the WEPP model. The photogrammetry-derived hydraulic radius can also be compared to hydraulic radius values estimated by the WEPP erosion model to see if the photogrammetry-derived hydraulic parameters significantly improve the erosion predictions.

TABLE 2. Regression coefficients for the power model of the rill density (D) vs. cross-sectional area (A) ($D = bA^c$) and the resultant rill spacing (Rspace)

WEPP plot	Location	Intercept b	Exponent c	Rspace (m)
31	Walnut Gulch, AZ	0.799	0.115	1.20
34	Walnut Gulch, AZ	0.495	0.220	0.69
72	Chickasha, OK	0.680	0.159	0.91
85	Woodward, OK	1.803	0.047	1.05
92	Woodward, OK	0.341	0.241	0.81
93	Woodward, OK	0.187	0.309	0.75
102	Sidney, MT	0.979	0.088	1.28
105	Sidney, MT	0.249	0.284	0.73
108	Meeker, CO	0.533	0.161	1.14
110	Meeker, CO	2.568	-0.296	1.57
114	Cottonwood, SD	0.983	0.934	1.21
116	Cottonwood, SD	1.278	0.082	1.04
120	Cottonwood, SD	1.810	0.063	0.89
121	Cottonwood, SD	0.971	0.183	0.50
127	Los Alamos, NM	1.040	0.072	1.41
131	Cuba, NM	0.892	0.118	1.04
134	Cuba, NM	0.829	0.117	1.14
138	Susanville, CA	0.683	0.186	0.70

Se = standard error of estimate
Sy = standard deviation of observed values
R = correlation coefficient

A numerical optimization procedure for calibrating complex models was used to obtain least squares estimates for three parameters: rill erodibility, interrill erodibility, and critical shear stress. This optimization model includes both Phase I and Phase II searches, which identify reasonable initial estimates of the unknowns and approach the point where the partial derivatives of the least squares objective function are zero, respectively. The WEPP erosion model was run in conjunction with the numerical optimization procedure with runoff and soil loss data from each of the 18 plots. Because the WEPP model is based on steady-state erosion equations, it should only be operated for steady-state conditions. In order to obtain a sufficient sample size for the optimization without compromising the model integrity, only the very wet rainfall run was used. The very wet run includes steady-state conditions at two rainfall fates plus either four or five periods where increasing rates of surface inflow were added at the upper end of the plot. This yields a total sample size of six or seven for each plot.

A summary of the statistical goodness-of-fit criteria of the erosion predictions on the 18 plots are presented in Table 3. The ratio of the standard error of estimate (Se) to the standard deviation (Sy) of the observed values was used as an index of goodness-of-fit, with a value of zero indicating a perfect fit and a value of 1 indicating that the model is no more accurate than using a simple mean; this ratio is useful because it provides for comparison with data for different flow rates. The values ranged from 0.05 to 1.09, with only one value greater than 1.0. Sixty-one percent of the ratios were less than 0.5, and 89% were less than 0.75; such results suggest that the calibrated model will produce accurate predictions. The correlation coefficients ranged from 0.72 to 0.999 on 17 of the 18 plots; the remaining value was zero. The bias values, which ranged from -1.7 to 0.87 g/s/m (grams per second per meter), and the mean observed sediment loss for each

TABLE 3. Goodness-of-fit statistics for the erosion rates predicted using the hydraulic parameters derived from the photogrammetric data

Plot	Se/Sy	R	Bias	Mean observed sediment loss (g/s/m)
31	0.39	0.95	-0.400	9.27
34	0.57	0.90	-0.490	12.34
72	0.49	0.93	0.022	1.79
85	0.05	0.999	-0.030	6.77
92	0.53	0.91	-0.140	4.12
93	0.37	0.95	0.100	4.08
102	0.51	0.91	-0.150	3.56
105	0.69	0.82	-0.460	3.63
108	0.35	0.96	-1.700	16.07
110	0.15	0.99	-0.080	8.86
114	0.48	0.93	0.025	5.33
116	0.20	0.99	-0.052	4.98
120	0.73	0.80	-0.110	3.70
121	0.89	0.72	-0.064	3.43
127	1.09	0	-0.360	2.84
131	0.36	0.96	-0.110	2.08
134	0.49	0.93	-0.140	2.24
138	0.27	0.98	0.087	4.25

Se = standard error of estimate
Sy = standard deviation of observed values
R = correlation coefficient

plot are also given in Table 3. Sixteen of the 18 values were negative, with the mean bias equal to -0.24. The mean bias, -0.24, is only 5.52 g/s/m, and therefore, the bias is assumed to be insignificant.

Overall, these statistics indicate that the calibrated hydraulic parameters lead to good predictive ability.

Comparison of Calibrated and Existing WEPP Predictions

As described previously, the WEPP erosion model contains a routine for estimating the hydraulic radius for a plot. Because the hydraulic radius is one of the flowpath characteristics of primary interest in this study, a comparison was made between the photogrammetrically derived values and the values estimated within the WEPP erosion model.

A plot (fig. 6) of the two estimates of the hydraulic radius on each of the 18 plots shows the wider scatter of data points about the 1:1 line. There is a clear tendency for the WEPP model to estimate greater hydraulic radius values than those determined with the photogrammetric data. The absolute relative error ranged from 8.5% to more than 500%, with a mean value of 66%.

Summary and Conclusions

While erosion rates are usually measured on a field-scale level, the erosion process occurs on a microscale level. Thus, a physically based model may achieve greater levels of accuracy and realism if it reflects the microscale level at which the erosion process begins. But to achieve this developmental objective, it is necessary to obtain physically based parameters from the microscale level. The hydraulic parameters calibrated as part of the overall WEPP objectives are based on microtopographic measurements. They appear to be a necessary part in the overall development of a physically based erosion model.

This study used low-altitude photogrammetric data to quantify rangeland surface hydraulic parameters not otherwise obtainable. The low-altitude photogrammetric data obtained in the WEPP rangeland field study provide an accurate and useful means of computing the hydraulic radius and flowpath density of a rangeland soil surface. This form of microtopographic data offers an extremely detailed characterization of the soil surface, which is particularly useful in low-relief rangeland areas. Although the expense and small-scale coverage limit its use to the research environment, photogrammetry serves an important function in calibrating models for estimating the hydraulic properties to be used in the development of a physically based model for estimating erosion rates from rangeland watersheds.

To develop a method for estimating the hydraulic parameters of rangeland watersheds, the contour data obtained from the low-altitude photogrammetry was transformed into computed cross-section data. For the photogrammetry data, comparisons were made to the cross-sections computed with the method developed herein. The method developed appears to be reliable for computing cross-sections for rangeland research plots.

Analyses with the cross-sectional data showed that the hydraulic radius required by the WEPP model could be estimated using the cross-sectional flowpath area. The latter can typically be computed from estimates of flow rates and runoff velocities. The flowpath density, which is another required input, was measured as a constant for each cross section. When the computed values of the hydraulic radius and flowpath density were used with the existing WEPP erosion model, they provided accurate estimates of erosion rates from 18 rangeland plots.

References

Drungil, C.E.C. 1989. Calibration based on photogrammetric analysis for a physically based rangeland erosion model. Ph.D. diss., University of Maryland, College Park.

Dymond, J.R. and D.L. Hicks. 1986. Steepland erosion measured from historical aerial photographs. *J. Soil and Water Conserv.* 41(4): 252-255.

Emmett, W.W. 1970. The hydraulics of overland flow on hillslopes. Geological Survey professional paper 662-A. Washington, DC: U.S. GPO.

Foster, G.R. (compiler). 1987. User requirements USDA Water Erosion Prediction Project (WEPP). NSERL Report 1, USDA-ARS, National Soil Erosion Research Laboratory, W. Lafayette, IN.

Lane, L.J. and M.A. Nearing. 1989. USDA-Water Erosion Prediction Project: Hillslope profile model documentation. NSERL Report No. 2, National Soil Erosion Research Laboratory, USDA-ARS, West Lafayette, IN.

Sanchez, C.E. and M.K. Wood. 1987. The relationship of soil surface roughness with hydrologic variables on natural and reclaimed range land in New Mexico. *Journal of Hydrology* 94: 345-354.

Simanton, J.R., L.R. West and M.A. Weltz. 1987. Rangeland experiments for water erosion prediction project. ASAE Paper No. 87-2545. St. Joseph, MI: ASAE.

Spomer, R.G. and R.L. Mahurin. 1984. Time-lapse remote sensing for rapid measurement of changing landforms. *J. Soil and Water Conserv.* 39(6): 397-401.

Swanson, N.P. 1965. Rotating-boom rainfall simulator. *Transactions of the ASAE* 8(1): 71-72.

Thomas, A.W. and R. Welch. 1988. Measurement of ephemeral gully erosion. *Transactions of the ASAE* 31(6): 1723-1728.

Thomas, A.W., R. Welch and T.R. Jordan. 1986. Quantifying concentrated-flow erosion on cropland with aerial photogrammetry. *J. Soil and Water Conserv.* 41(4): 249-252.

Welch, R., T.T. Jordan and A.W. Thomas. 1984. A photogrammetric technique for measuring soil erosions. *Oil and Water Conserv.* 39(3): 191-194.

Wischmeier, W.H. and D.D. Smith. 1978. Predicting rainfall erosion losses - A guide to conservation planning. U.S. Department of Agriculture Handbook No. 537.